FIRST MEASUREMENT OF A RAPID INCREASE IN THE AGN FRACTION IN HIGH-REDSHIFT CLUSTERS OF GALAXIES

Jason Eastman[1], Paul Martini[1], Gregory Sivakoff[1], Daniel D. Kelson[2], John S. Mulchaey[2], and Kim-Vy Tran[3,4]
ApJL Accepted [1 June 2007]

ABSTRACT

We present the first measurement of the AGN fraction in high-redshift clusters of galaxies ($z \sim 0.6$) with spectroscopy of one cluster and archival data for three additional clusters. We identify 8 AGN in all four of these clusters from the *Chandra* data, which are sensitive to AGN with hard X-ray (2-10keV) luminosity $L_{X,H} > 10^{43}$ erg s^{-1} in host galaxies more luminous than a rest frame $M_R < -20$ mag. This stands in sharp contrast to the one AGN with $L_{X,H} > 10^{43}$ erg s^{-1} we discovered in our earlier study of eight low-redshift clusters with $z = 0.06 \rightarrow 0.31(\bar{z} \sim 0.2)$. Three of the four high-redshift cluster datasets are sensitive to nearly $L_{X,H} > 10^{42}$ erg s^{-1} and we identify seven AGN above this luminosity limit, compared to two in eight, low-redshift clusters. Based on membership estimates for each cluster, we determine that the AGN fraction at $z \sim 0.6$ is $f_A(L_X > 10^{42}; M_R < -20) = 0.028^{+0.019}_{-0.012}$ and $f_A(L_X > 10^{43}; M_R < -20) = 0.020^{+0.012}_{-0.008}$. These values are approximately a factor of 20 greater than the AGN fractions in lower-redshift ($\bar{z} \sim 0.2$) clusters of galaxies and represent a substantial increase over the factors of 1.5 and 3.3 increase, respectively, in the measured space density evolution of the hard X-ray luminosity function over this redshift range. Potential systematic errors would only increase the significance of our result. The cluster AGN fraction increases more rapidly with redshift than the field and the increase in cluster AGN indicates the presence of an AGN Butcher-Oemler Effect.

Subject headings: galaxies: active – galaxies:evolution – clusters: individual (MS2053-04, CL0542-4100, CL0848.6+4453, CL0016+1609)

1. INTRODUCTION

Measurements of AGN in low-redshift clusters of galaxies have received substantial recent interest because of their apparent importance for regulating the heating of the intracluster medium (McNamara et al. 2000; Fabian et al. 2000) and the efficiency with which sensitive *Chandra* observations can identify the relatively rare AGN population in clusters. In recent work Martini et al. (2006) showed that the X-ray selected AGN in clusters was 5% (for 0.5-8keV $L_X > 10^{41}$ erg s^{-1} in galaxies above $M_R < -20$ mag), or five times as many as found via emission-line selection in purely spectroscopic surveys (Dressler et al 1985). These observations also demonstrated that the excess X-ray point source surface density observed toward the fields of clusters of galaxies (e.g. Lazzati et al. 1998; Cappi et al. 2001; Sun & Murray 2002) were due to X-ray emission from cluster members and not chance associations.

The high-redshift cluster AGN population has been less well studied due to the absence comparably-sensitive *Chandra* observations of $z > 0.5$ clusters and the greater difficulty of spectroscopic follow-up. Nevertheless, AGN are expected to be more common in higher-redshift clusters because of the overall increase in the AGN space density at high redshift (e.g. Osmer 2004) and the increase in the fraction of star forming galaxies in clusters at higher redshift (e.g. Postman et al. 2001), which indicates that high-redshift cluster galaxies are richer in cold gas than their lower-redshift

counterparts. Observations of several high-redshift clusters have also found substantial AGN populations in some clusters (Dressler & Gunn 1983; Johnson et al. 2003, 2006), while surface density studies have found evidence for an increase in the X-ray source surface density at high redshift (Dowsett 2005). Feedback from cluster AGN could also play a substantial role in shutting down star formation in cluster galaxies, such as illustrated by the significant decrease in blue galaxies found by Butcher & Oemler (1978).

In this *Letter* we present the first measurement of the cluster AGN fraction at high redshift ($z \sim 0.58$) from analysis of four archival *Chandra* observations, our spectroscopic observations of one cluster (MS2053-04), and literature data for three additional clusters (CL0016+1619 at $z = 0.5466$; CL0542-4100 at $z = 0.630$; CL0848.6+4453 at $z = 0.57$). These observations reveal a substantial increase in the cluster AGN fraction at high redshift, which has many implications for the preheating of the ICM during cluster assembly, downsizing in the AGN population as a function of environment, and the AGN contribution to X-ray studies of high-redshift clusters for cosmological studies.

2. OBSERVATIONS

We have identified AGN in MS2053-04 via spectroscopic observations of X-ray counterparts from archival *Chandra* observations. MS2053-04 has been observed twice with *Chandra* (ObsID 551 and 1667), which are a pair of 45ks ACIS-I observations that partially overlap one another (both include the cluster core). The area of the first of these datasets was imaged with deep *BVRI* observations with the Tek5 CCD camera at the 2.5m du Pont telescope at Las Campanas Observatory in September 2002 (the second *Chandra* dataset was not yet public). These images were processed and galaxies identified and matched to the X-ray observations following the procedures described in Martini et al. (2006).

[1] Department of Astronomy, The Ohio State University, 140 W. 18th Ave., Columbus, OH 43210; jdeast,martini,sivakoff@astronomy.ohio-state.edu

[2] Carnegie Observatories, 813 Santa Barbara Street, Pasadena, CA 91101-1292; kelson,mulchaey@ociw.edu

[3] Leiden Observatory, Niels Bohrweg 2, 2333 CA Leiden, The Netherlands; kimvy.tran@gmail.com

[4] Institute for Theoretical Physics, University of Zürich, CH-8057 Zürich, Switzerland
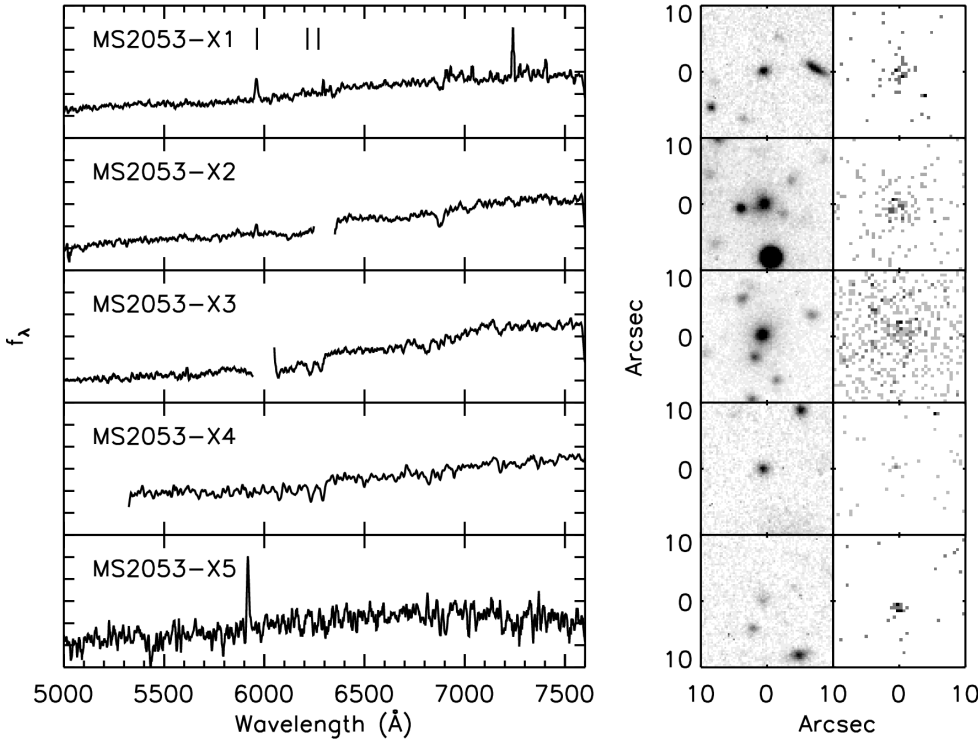
FIG. 1.— Spectra (*left*), *R*–band image (*middle*), and X-Ray image (*right*) of X-ray sources in MS2053-04. The gaps in the spectra correspond to the gaps between the chips of the IMACS CCDs. Redshifted [OII] $\lambda 3727$ is present in X1, X2, and X5, but not X4, while this wavelength falls in a chip gap for X3. Ca H & K can be seen in X3 and X4, but not in X1 or X5 and falls on the chip gap for X2. The location of the redshifted [OII] and Ca H & K are indicated in the top panel.

This analysis identified 82 X-ray sources with visible-wavelength counterparts and these were used to design slit masks for the IMACS spectrograph (Dressler et al. 2006) on the 6.5m Walter Baade Telescope of the Magellan Project. A total of four, multi-tier slit masks were designed with approximately 180 objects per mask; however, faint sources were assigned to multiple masks and therefore a total of 617 unique objects were observed. These objects included all X-ray counterparts brighter than $I \leq 23.5$ mag. Additional sources were prioritized by I magnitude to obtain information about the inactive cluster galaxy population. Color and image quality constraints were not employed to pre-select potential cluster members due to the small expected size of typical cluster members and the large population of relatively blue or Butcher-Oemler galaxies in this high-redshift cluster.

The four slit masks were observed in August 2004 for three hours each and these data were processed into 2-D spectra with the COSMOS package[5]. 1-D spectra were extracted with the IRAF APALL package and redshifts were measured with a modified version of the Sloan Digital Sky Survey pipeline, although each was also inspected by eye. This identified a total of 41 counterparts to X-ray sources, including four at the cluster redshift. To supplement these observations and obtain improved flux measurements we reprocessed the original *Chandra* data and added the second ACIS-I pointing. These data were processed with CIAO 3.3.0.1[6], CALDB 3.2.4 and NASA's FTOOLS 6.1.1[7]. Individual X-ray sources were iden-

tified with the CIAO WAVDETECT algorithm from both the individual observations and a merged version of the observations. This analysis reidentifed the four X-ray counterparts at the cluster redshift. We also cross-correlated these X-ray sources with a spectroscopic study by Tran et al. (2005) and identified one additional X-ray source at the cluster redshift. The properties of these five sources are provided in Table 1.

3. RESULTS

We have identified a total of five X-ray counterparts at the redshift of MS2053-04, although we only classify the one AGN within r_{200} as a member. The AGN classification is based on the rest-frame, hard X-ray luminosity [2-10 keV] of $L_{X,H} = 10^{42}$ erg s^{-1} (measured on the merged datasets). Of the remaining four X-ray counterparts, one is associated with the Brightest Cluster Galaxy (BCG). This source is coincident with the peak of the X-ray emission from the intracluster medium and evidence for an additional, AGN component is inconclusive (see also Tran et al. 2005). The three remaining X-ray counterparts lie outside the cluster's projected r_{200} radius of 1.5 Mpc, which we calculated from the cluster's velocity dispersion (Carlberg et al. 1997; Treu et al. 2003) of $\sigma = 865$ km s^{-1} (Tran et al. 2005). While they may be bound to the cluster, we adopt the projected radius of r_{200} to compare measurements of the AGN fraction between clusters. Figure 1 presents the visible-wavelength spectra, *R*–band images, and X-ray images of all five of the X-ray sources at the redshift of MS2053-04.

3.1. *The AGN Fraction in MS2053-04*

---

[5] http://www.ociw.edu/Code/cosmos

[6] http://asc.harvard.edu/ciao/

[7] http://heasarc.gsfc.nasa.gov/docs/software/lheasoft/

TABLE 1
X-RAY SOURCES AT MS2053-04 REDSHIFT

Name	Object ID	I	V-I	$\log L_{X,H}$	z	R [Mpc]	R/r_{200}	Notes
MS2053-X1	CXOU J205647.1-044407	21.26 (0.05)	0.950 (0.08)	$42.80^{+0.15}_{-0.12}$	0.600	3.57	2.35	Not in 1st X-Ray Field
MS2053-X2	CXOU J205617.1-044155	18.96 (0.05)	2.020 (0.08)	$42.81^{+0.10}_{-0.08}$	0.600	1.67	1.10	
MS2053-X3	CXOU J205621.2-043749	19.20 (0.05)	2.048 (0.08)	$42.43^{+0.20}_{-0.16}$	0.584	0	0	BCG (likely not an AGN)
MS2053-X4	CXOU J205621.2-043552	21.35 (0.05)	1.774 (0.08)	$42.03^{+0.29}_{-0.20}$	0.585	0.78	0.51	z from Tran et al. (2005)
MS2053-X5	CXOU J205608.1-043211	22.73 (0.05)	0.421 (0.08)	$42.59^{+0.20}_{-0.15}$	0.588	2.59	1.71	

NOTE. — AGN in MS2053-04 ($z = 0.583$). The columns include: (1) our identifier; (2) full name; (3) I−band magnitude; (4) $V - I$ color; (5) log of the hard X-ray luminosity; (6) redshift; (7) projected distance from the cluster center in Mpc; (8) projected distance relative to r_{200}; (9) notes about the X-ray source.

TABLE 2
KNOWN AGN IN HIGH-REDSHIFT CLUSTERS

Object ID	z	$\log L_{X,H}$	R/R_{200}	Refs
CL0016+1619				
E 0015+162	0.553	45.48	0.31	a
CXOMP J001842.0+163425	0.55	42.59	0.80	b
CL0542-4100				
CXOMP J054240.8-405626	0.639	43.59	0.40	b
CXOMP J054255.0-405922	0.644	43.00	0.12	b
CXOMP J054251.4-410205	0.637	43.27	0.21	b
CXOMP J054248.2-410140	0.634	43.16	0.17	b
CXOMP J054259.5-410241	0.638	43.29	0.33	b
CL0848.6+4453				
CXOSEXSI J084837.5+445710	0.569	42.9	0.34	c
CXOSEXSI J084843.2+445806	0.566	42.6	0.34	c
CXOSEXSI J084846.0+445945	0.567	43.1	0.62	c
CXOSEXSI J084858.0+445434	0.573	43.8	0.46	c
CXOSEXSI J084931.3+445549	0.567	42.9	1.49	c

NOTE. — AGN in three additional, high-redshift clusters from the literature: CL0016+1609 ($z = 0.5466$); CL0542-4100 ($z = 0.630$); CL0848.6+4453 (0.57). For each AGN in column (1) we list: (2) the redshift; (3) log of the hard X-ray luminosity; (4) projected distance from the cluster center relative to r_{200}; (5) references are: (a) Margon et al. (1983); (b) Silverman et al. (2005); (c) Eckart et al. (2006).

Calculation of the AGN fraction in MS2053-04 requires measurement of the number of cluster members without luminous X-ray counterparts. Following the AGN fraction measurement of Martini et al. (2006), we choose to estimate the number of cluster members above a rest-frame $M_R < -20$ mag, which corresponds to $I = 22.4$ mag for an evolved stellar population at this redshift. As our spectroscopic catalog is not complete for all galaxies to this magnitude limit, we instead use the efficiency of our spectroscopic identification of cluster members, the surface density of resolved, $I \le 22.4$ mag objects, and the membership data collected by Tran et al. (2005) to estimate the total cluster galaxy population. We calculate this efficiency for the full sample, as a function of magnitude, and as a function of color and estimate the cluster galaxy population N_{est} within r_{200} is 66 (no binning), 74 (color binning), or 66 (magnitude binning). From this analysis we conclude that there are approximately 66 galaxies brighter than $M_R < -20$ mag in the cluster.

3.2. Literature data and the Evolution of Cluster AGN

We searched the *Chandra* archive and the literature to identify additional clusters at $z \sim 0.6$ with both comparably sensitive observations and spectroscopic observations of the X-ray sources and identified three clusters: CL0016+1609 ($z = 0.5466$, 61ks) and CL0542-4100 ($z = 0.630$, 51ks), where X-ray sources in these fields had been targeted by
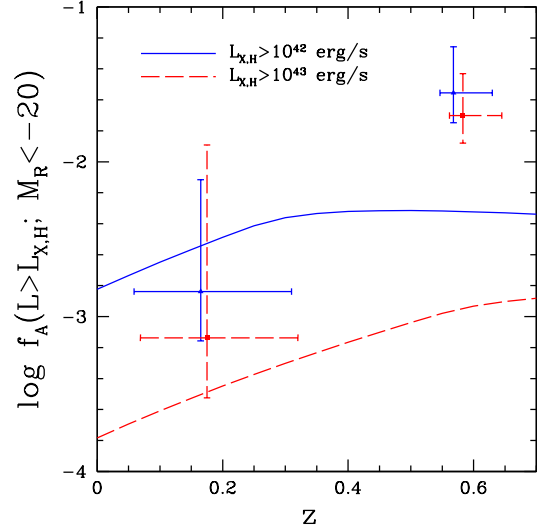

FIG. 2.— Evolution of the cluster AGN fraction with redshift. Cluster AGN with $L_{X,H} > 10^{42}$ erg s^{-1} (*blue triangles*) and $L_{X,H} > 10^{43}$ erg s^{-1} (*red squares*) are more common at $\bar{z} \sim 0.6$ than in the low-redshift ($\bar{z} \sim 0.2$) sample of eight clusters studied by (Martini et al. 2006). The redshift range of the clusters used is marked by the error bars. The evolution is also more pronounced than expected from integration of the Ueda et al. (2003) HXLF.

the ChaMP survey (Kim et al. 2004; Silverman et al. 2005) and CL0848.6+4453 (0.57, 185ks), which has been targeted by the SEXSI survey (Harrison et al. 2003; Eckart et al. 2006). In addition, CL0016+1609 has extensive membership data and a measured velocity dispersion of $\sigma = 1234$ km s^{-1} (Dressler & Gunn 1992; Carlberg et al. 1996; Ellingson et al. 1998). From these membership data and the reported completeness of the CNOC survey, we estimate that there are approximately 200 cluster members more luminous than $M_R = -20$ mag in CL0016+1609. The other two clusters in this sample, CL0542-4100 and CL0848.5+4453, do not have substantial spectroscopic data outside of the X-ray counterparts. For these clusters, we use the measured X-ray temperatures of 7.9 keV (Xue & Wu 2000) and 3.6 keV (Holden et al. 2001), respectively, to estimate velocity dispersions of $\sigma = 1200$ km s^{-1} and 670 km s^{-1}. We then use the relationship between velocity dispersion and cluster richness N_{gals} from the MAXBCG survey (Koester et al. 2007) to estimate the number of members brighter than $M^* + 1$, or approximately our galaxy absolute magnitude threshold. From their fitting formula we estimate that there are 152 members in CL0542-4100 and 24 in CL0848.5+4453. This relation also predicts 55 members in MS2053-04 and 172 members in CL0016+1609 and these values are agree with our previous estimates to within 20%. We adopt these membership values

for all four clusters to consistently calculate the AGN fraction; we discuss the uncertainties in this assumption below.

Our observations of MS2053-04, along with those for CL0016+1619 and CL0848.6+4453, are approximately deep enough to detect sources to a limiting rest-frame hard X-ray luminosity of $L_{X,H} > 10^{42}$ erg s^{-1}. In these three clusters we have identified a total of seven AGN within r_{200} in a total population of 251 galaxies. For comparison, we identified only two AGN above this limit in a sample of eight low-redshift ($\bar{z} \sim 0.2$) clusters with a total of 1377 cluster galaxies (Martini et al. 2007). At $\bar{z} \sim 0.6$, we therefore find the AGN fraction is $f_A(L_{X,H} > 10^{42}; M_R < -20) = 0.028^{+0.019}_{-0.012}$ (7 AGN divided by 251 cluster galaxies). The quoted uncertainties correspond to 90%, one-sided Poisson confidence limits. The data for the highest-redshift cluster in our sample (CL0542-4100) is only sensitive to AGN more luminous than $L_{X,H} > 10^{43}$ erg s^{-1} and there are a total of eight AGN within r_{200} above this limit in these four clusters (with an estimated $\sim$ 400 total cluster members), in striking contrast to the presence of only one comparably luminous AGN in eight low-redshift clusters. For this X-ray luminosity threshold we estimate that the AGN fraction is $f_A(L_{X,H} > 10^{43}; M_R < -20) = 0.020^{+0.012}_{-0.008}$. In contrast, at $\bar{z} = 0.2$ the AGN fractions from Martini et al. (2007) are $f_A(L_{X,H} > 10^{42}; M_R < -20) = 0.0015^{+0.0024}_{-0.0011}$ and $f_A(L_{X,H} > 10^{43}; M_R < -20) = 0.0007^{+0.0021}_{-0.0007}$, or approximately a factor of 20 lower. Figure 2 plots the cluster AGN fraction for these two luminosity thresholds at low and high redshift and illustrates the significant increase in the cluster AGN fraction at high-redshift compared to the lower-redshift sample. For comparison, we also show the relative evolution of the integrated space density of AGN above these two luminosity thresholds from the parameterization of Ueda et al. (2003). While the overall normalization of the curves is arbitrary, the relative evolution of the $L_{X,H} > 10^{42}$ erg s^{-1} and $L_{X,H} > 10^{43}$ erg s^{-1} samples are not. These curves indicate the cluster AGN fraction increases more rapidly with lookback time than the AGN space density in the field. Specifically, the field AGN space density increases by only a factor of 1.5 from $z \sim 0.2$ to $z \sim 0.6$ for $L_{X,H} > 10^{42}$ erg s^{-1} and only a factor of 3.3 for $L_{X,H} > 10^{43}$ erg s^{-1}, compared to the factor of ~ 20 we observe in clusters. While there is substantial variation between the AGN fraction of individual clusters, if we exclude CL0848, the largest contributor to the AGN fraction, and redo the calculation, we still see a factor of 10 increase in the AGN space density.

While the substantial evolution in the AGN fraction in clusters is due to small numbers of AGN, it is measured from a large population of inactive cluster galaxies. The measured fractions at low and high redshift are formally inconsistent with the 90%, one-sided confidence intervals. At high redshift we have more AGN and consequently have a more significant measure of the AGN fraction. We therefore use these measurements of the high-redshift AGN fraction and a binomial probability distribution to ask the probability of detecting 2 AGN with $L_{X,H} > 10^{42}$ erg s^{-1} or 1 with $L_{X,H} > 10^{43}$ erg s^{-1} in the low-redshift sample and calculate that the probability (for each) is less than 1%. The main systematic error in these calculations is in the number of galaxies brighter than $M_R < -20$ mag in each cluster. The detailed membership information for MS2053-04 (Tran et al. 2005) and CL0016+1619 (Dressler & Gunn 1992; Ellingson et al. 1998) suggest there are 66 and 200 members in these clusters, respectively, and both of these values agree to within

20% with the richness – velocity dispersion relationship from Koester et al. (2007). This suggests that systematic errors in membership are insignificant compared to the observed evolution in the AGN fraction. Two additional sources of uncertainty in these estimates are galaxy luminosity evolution between $z \sim 0.6$ and $z \sim 0.2$ and the actual sensitivity and completeness of the *Chandra* datasets. First, M_R^* is approximately 0.4 mag brighter at $z \sim 0.6$ than $z \sim 0.2$. Our fixed luminosity threshold extends further below M_R^* at high redshift and therefore we have overestimated the cluster membership (relative to M^*) at higher redshift and underestimated the AGN fraction. Secondly, the *Chandra* observations are not be uniformly sensitive to our adopted thresholds of $L_{X,H} > 10^{42}$ erg s^{-1} and $L_{X,H} > 10^{43}$ erg s^{-1}, such as the fact that the 61ks observation of CL0016+1609 is shallower than the 90ks of total integration time available for the center of MS2053-04. We estimate the size of this effect by calculating the approximate depth of each *Chandra* exposure and integrating the hard X-ray luminosity function of Ueda et al. (2003) from the current depth to $L_{X,H} > 10^{42}$ erg s^{-1}. This exercise indicates that we may expect as many as 50% more AGN if these data were uniformly sensitive to $L_{X,H} > 10^{42}$ erg s^{-1} sources. Two final points are that the spectroscopy of all X-ray sources may not be complete and it is difficult to unambiguously identify an AGN in the BCG due to the substantial X-ray emission from the ICM. All of these potential systematic effects would increase the AGN fraction and strengthen our result.

4. SUMMARY

We have analyzed archival *Chandra* observations of four high-redshift $z \sim 0.6$ clusters of galaxies to derive the first measurement of the cluster AGN fraction at high redshift. Our spectroscopic observation of the $z = 0.586$ cluster MS2053-04 identified one cluster AGN with a rest-frame, hard X-ray luminosity $L_{X,H} > 10^{42}$ erg s^{-1}, while when we include spectroscopic observations from the literature we find a total of eight AGN with $L_{X,H} > 10^{43}$ erg s^{-1} in four clusters and seven with $L_{X,H} > 10^{42}$ erg s^{-1} in the three clusters with longer *Chandra* observations. We use our spectroscopic survey of inactive galaxies in MS2053-04, literature data for CL0016, and simple scaling arguments to estimate the total number of inactive galaxies in each cluster above a rest-frame luminosity of $M_R < -20$ mag to estimate the AGN fraction in clusters above these two hard X-ray luminosity thresholds: $f_A(L_{X,H} > 10^{42}; M_R < -20) = 0.028^{+0.019}_{-0.012}$ and $f_A(L_{X,H} > 10^{43}; M_R < -20) = 0.020^{+0.012}_{-0.008}$.

Although these estimates correspond to a small fraction of the total cluster galaxy population, they represent a substantial increase over the measured cluster AGN fraction at low-redshift. Specifically, in a sample of eight clusters of galaxies with an average redshift of $z \sim 0.2$ Martini et al. (2006) measured only one AGN with $L_{X,H} > 10^{43}$ erg s^{-1} and only two AGN with $L_{X,H} > 10^{42}$ erg s^{-1}. From these measurements we find that the cluster AGN fraction has increased by approximately a factor of 20 for these two hard X-ray luminosity thresholds between $\bar{z} \sim 0.2$ and $\bar{z} \sim 0.6$. This evolution corresponds to a significantly greater increase in the cluster AGN population at high-redshift than the measured evolution of the field hard X-ray LF by Ueda et al. (2003) over the same redshift range and points to the existence of an "AGN Butcher-Oemler Effect" in clusters of galaxies. The overdensity of AGN at high redshift could be an additional source of preheating of the ICM during cluster assembly, has important

cosmological implications for X-ray studies of high-redshift clusters, and could show how the environment influences the AGN population.

Facility: du Pont (Tek No. 5 imaging CCD, WFCCD), Magellan:Baade (IMACS imaging spectrograph)

REFERENCES

Beers, T. C., Flynn, K., & Gebhardt, K. 1990, AJ, 100, 32
Butcher, H. & Oemler, A. 1978, ApJ, 219, 18
Cappi, M., et al. 2001, ApJ, 548, 624
Carlberg, R.G. et al. 1996, ApJ, 462, 32
Carlberg, R. G., Yee, H. K. C., & Ellingson, E. 1997, ApJ, 478, 462
Dowsett, R. 2005, Ph.D. Thesis
Dressler, A. & Gunn, J.E. 1983, ApJ, 270, 7
Dressler, A., Thompson, I. B., & Schectman, S. A., 1985, ApJ, 288, 481
Dressler, A. & Gunn, J.E. 1992, ApJS, 78, 1
Dressler, A., Hare, T., Bigelow, B.C., Osip, D.J. 2006, Proc. SPIE Vol. 6269, 13
Eckart, M.E. et al. 2006, ApJS, 165, 19
Ellingson et al. 1998, ApJS, 116, 247
Fabian, A.C., 2000, MNRAS, 318, L65
Gehrels, N., 1986, ApJ, 303, 336G
Gisler, G.R. 1978, MNRAS, 183, 633
Harrison, F.A., Eckart, M.E., Mao, P.H., Helfand, D.J., & Stern, D. 2003, ApJ, 596, 944
Holden, B.P. et al. 2001, ApJ, 122, 629
Jeltema, T. E., Mulchaey, J. S., Lubin, L. M., Rosati, P., & Böhringer, H., 2006, ApJ, 649, 649
Johnson, O., Best, P. N., & Almaini, O., MNRAS, 343, 924
Johnson, O., et al. 2006, MNRAS, 371, 1777

Kim, D. W., et al. 2004, ApJS, 150, 19
Koester, B. P., et al. 2007, ApJS, *accepted*, (astro-ph/0701268)
Lazzati D., Campana S., Rosati P., Chincarini G., & Giacconi R., 1998 A&A, 331, 41
Margon, B., Spinrad, H., & Downes, R.A. 1983, Nature, 301, 221
Martini, P., Kelson, D. D., Mulchaey, J. S., & Trager, S. C. 2002, ApJ, 576, L109
Martini, P., Kelson, D. D., Kim, E., Mulchaey, J. S., & Athey, A. A. 2006, ApJ, 644, 116
Martini, P., Mulchaey, J. S., & Kelson, D. D. ApJ, *submitted*
McNamara, B.R., et al., 2000, ApJ, 534, L135
Osmer, P. S. 2004, in Coevolution of Black Holes and Galaxies, ed L. C. Ho, 324
Postman, M., Lubin, L.M., & Oke, J.B. 2001, AJ, 122, 1125
Silverman, J.D. et al. 2005, ApJ, 618, 123
Sun, M., & Murray, S. S. 2002, ApJ, 577, 139
Tran, K. H., van Dokkum, P., Illingworth, G. D., Kelson, D.; Gonzalez, A., & Franx, M. 2005, ApJ, 619, 134T
Treu, T., et al. 2003, ApJ, 591, 53
Ueda, Y., Akiyama, M., Ohta, K., and Miyaji, T. 2003, ApJ, 598, 886
Xue, Y.-J. & Wu, X.-P. 2000, ApJ, 538, 65